

One-dimensional atom laser in microgravity

Yi Qin(秦毅), Xiaoyang Shen(沈晓阳), and Lin Xia(夏林)

Citation: Chin. Phys. B, 2021, 30 (**11**): 110306. DOI: 10.1088/1674-1056/abff25
Journal homepage: http://cpb.iphy.ac.cn; http://iopscience.iop.org/cpb

What follows is a list of articles you may be interested in

Classical-field description of Bose-Einstein condensation of parallel light in a nonlinear optical cavity

Hui-Fang Wang(王慧芳), Jin-Jun Zhang(张进军), and Jian-Jun Zhang(张建军)
Chin. Phys. B, 2021, 30 (**11**): 110301. DOI: 10.1088/1674-1056/abf4f9

Ultradilute self-bound quantum droplets in Bose-Bose mixtures at finite temperature

Jia Wang(王佳), Xia-Ji Liu(刘夏姬), and Hui Hu(胡辉)
Chin. Phys. B, 2021, 30 (**1**): 010306. DOI: 10.1088/1674-1056/abd2ad

Effects of a finite number of particles on the thermodynamic properties of a harmonically trapped ideal charged Bose gas in a constant magnetic field

Duan-Liang Xiao(肖端亮), Meng-Yun Lai(赖梦云), Xiao-Yin Pan(潘孝胤)
Chin. Phys. B, 2016, 25 (**1**): 010307. DOI: 10.1088/1674-1056/25/1/010307

Spin-orbit coupled Bose-Einstein condensates with Rydberg-dressing interaction

Lü Hao, Zhu Shao-Bing, Qian Jun, Wang Yu-Zhu
Chin. Phys. B, 2015, 24 (**9**): 090308. DOI: 10.1088/1674-1056/24/9/090308

The effect of s-wave scattering length on self-trapping and tunneling phenomena of Fermi gases in one-dimensional accelerating optical lattices

Jia Wei, Dou Fu-Quan, Sun Jian-An, Duan Wen-Shan
Chin. Phys. B, 2015, 24 (**4**): 040307. DOI: 10.1088/1674-1056/24/4/040307

One-dimensional atom laser in microgravity*

Yi Qin(秦毅)[1,2], Xiaoyang Shen(沈晓阳)[1,2], and Lin Xia(夏林)[1,3,†]

[1] *Beijing National Laboratory for Condensed Matter Physics, Institute of Physics, Chinese Academy of Sciences, Beijing* 100190, *China*
[2] *University of Chinese Academy of Sciences, Beijing* 100049, *China*
[3] *Songshan Lake Materials Laboratory, Dongguan* 523808, *China*

(Received 15 March 2021; revised manuscript received 19 April 2021; accepted manuscript online 8 May 2021)

Using coupled Gross–Pitaevksii (GP) equations, we simulate the output of one-dimensional pulsed atom laser in space station. We get two atom laser pulses propagating in opposite directions with one pulsed RF coupling. Compared with atom laser under gravity, the laser pulse in microgravity shows much slower moving speed, which is suitable to be used for long-term investigations. We also simulate the output flux at different coupling strengths.

Keywords: microgravity, atom laser, Bose–Einstein condensation

PACS: 03.75.Pp, 03.75.Kk, 03.75.Nt, 03.75.Mn **DOI:** 10.1088/1674-1056/abff25

1. Introduction

Recently, the Bose–Einstein condensation (BEC) is created in space station for the first time.[1] In the other experiment, an atomic clock is running in space station.[2] Under microgravity environment in space station, longer investigation time and colder atom clouds can be achieved, which are crucial for precision measurements and quantum physics studies.[1–6] The subnanokelvin BEC with one second free expansion time has been realized in microgravity.[1,4] In an Earth-orbiting research laboratory, one group performed manipulation of multi-components BEC experiment in the flight.[4] Theories and simulations in microgravity have been studied too. The simulation of three-dimensional (3D) atom laser in microgravity with isotropic output density distribution has been explored.[7] BECs in bubble geometry,[8] sphere surface,[9] and shell geometry[10,11] have been proposed.

The invention of optical laser has great impact on science and technology. However, the diffraction limit hinders the application of laser in precision measurements. Shorter wavelength of matter wave compared with photon means atom laser can go beyond the diffraction limit of light. BEC under ultra low temperature makes realization of atom laser possible. In 1997, the MIT group first realized atom laser.[12] The team transferred atoms from a trapped state into an untrapped state by use of a short radio frequency (RF) pulse in spinor BEC. Later, properties about the intensity fluctuation,[13,14] outcoupled rate,[15] divergence of the beam,[16] spatial and temporal coherence[17–22] of atom laser have been analyzed. Like optical lasers, atom lasers have great application potential in the field of precision measurements.[23]

Temperature and coherence time are the critical factors limit the measurement precision.[15] Due to gravity, the output velocity is too fast and the coherence time of atom laser is less than one second. Several groups performed experiments with cancellation of gravity[24] or mimic the environment of free fall[25] although the investigation time are not able to be as long as in space.

Particularly, many-body system shows different properties between 3D and one-dimension (1D). One-dimensional interacting boson system in Tonks–Girardeau (TG) regime[26,27] in which the interaction energy is much larger than the kinetic energy, the two bosons could not occupy the same position just like fermions. In TG regime, the wavefunction of interacting bosons is the same with the non-interacting fermions. The prediction about TG gas in equilibrium and its fermionization behavior has been realized by use of ultracold atoms in optical lattices.[27] Recently, the dynamical fermionization and the bosonic–fermionic oscillation of TG gas are observed in experiments.[28] Besides, the collision experiment of one-dimensional interacting bosons reveals the invalid of ergodic hypothesis in many-body system. This phenomenon is called quantum Newton's cradle.[29] Thus, novel behaviors may occur in one-dimensional spinor BEC is one of our motivations to explore atom laser in one dimension.

In this paper, we study one-dimensional pulsed atom laser in microgravity. Three properties have been found. (i) The atom laser evolves in both directions in microgravity in contrast to the one direction propagation of atom laser in gravity. (ii) Compared with atom laser in gravity, the moving veloc-

*Project supported by the National Key Research and Development Program of China (Grant Nos. 2016YFA0300600 and 2016YFA0301500) and the National Natural Science Foundation of China (Grant No. 11874418).

†Corresponding author. E-mail: linxia@iphy.ac.cn

© 2021 Chinese Physical Society and IOP Publishing Ltd

ity of output beam is drastically reduced. (iii) The coupling strengths has the same effect both in gravity and in microgravity. The output atoms population changes drastically as the coupling strength changes. Our study is able to give a guide for the future experiments in space station.

2. Model for atom laser

We consider the system of ^{87}Rb $F = 2$ manifold coupled by RF field.[15,30] In weak magnetic field, the energy level splitting is equal. The Zeeman sublevels are coupled when RF pulse is applied. The magnetically trapped states are $|F = 2, m_F = 2\rangle$ and $|F = 2, m_F = 1\rangle$. The anti-trapped states are $|F = 2, m_F = -1\rangle$ and $|F = 2, m_F = -2\rangle$. Atoms in anti-trapped states are repelled by magnetic potential. The untrapped state is $|F = 2, m_F = 0\rangle$. Untrapped state feels only gravitational potential and mean field interaction. RF field couples all of these sublevels so usually the anti-trapped states are weakly populated. For the main results in this paper, the sum of the occupation atom number of anti-trapped states is negligible. Under gravity, the potential minimum of trapped states are shifted. In microgravity, trapped states have the same equilibrium positions.

The Gross–Pitaevksii (GP) equation is suitable for investigating pulsed atom laser.[15,30] It captures all the main results of atom laser. We use the effective one-dimensional GP model.[15,30] The GP model is given by

$$
\begin{aligned}
\mathrm{i}\dot{\psi}_2 &= \left(-\frac{1}{2}\frac{\partial^2}{\partial y^2} + y^2 + 2\Delta - Gy + U||\psi||^2\right)\psi_2 + 2\Omega\psi_1,\\
\mathrm{i}\dot{\psi}_1 &= \left(-\frac{1}{2}\frac{\partial^2}{\partial y^2} + \frac{1}{2}y^2 + \Delta - Gy + U||\psi||^2\right)\psi_1\\
&\quad + 2\Omega\psi_2 + \sqrt{6}\Omega\psi_0,\\
\mathrm{i}\dot{\psi}_0 &= \left(-\frac{1}{2}\frac{\partial^2}{\partial y^2} - Gy + U||\psi||^2\right)\psi_0\\
&\quad + \sqrt{6}\Omega\psi_1 + \sqrt{6}\Omega\psi_{-1},\\
\mathrm{i}\dot{\psi}_{-1} &= \left(-\frac{1}{2}\frac{\partial^2}{\partial y^2} - \frac{1}{2}y^2 - \Delta - Gy + U||\psi||^2\right)\psi_{-1}\\
&\quad + 2\Omega\psi_{-2} + \sqrt{6}\Omega\psi_0,\\
\mathrm{i}\dot{\psi}_{-2} &= \left(-\frac{1}{2}\frac{\partial^2}{\partial y^2} - y^2 - 2\Delta - Gy + U||\psi||^2\right)\psi_{-2}\\
&\quad + 2\Omega\psi_{-1}, \qquad (1)
\end{aligned}
$$

where $||\psi||^2 = \sum_{m=-2}^{2}|\psi_m|^2$, $m = -2, -1, 0, 1, 2$ are the magnetic quantum numbers. The dimensionless two-body interaction coefficient

$$U = \frac{2}{3}\left(\frac{\omega_{1z}}{\omega_{1y}}\right)^{3/5}\left(\frac{15Na_0}{a_{1y}}\right)^{3/5}|m_{\mathrm{trap}}|^{2/5},$$

derived by requiring that the three-dimensional chemical potential equals the one-dimensional one within Thomas Fermi approximation. N is the total atom number, and ω_{1y} is the trapping frequency along gravity direction of $|F = 2, m_F = 1\rangle$. $a_{1y} = \sqrt{\hbar/(M\omega_{1y})}$, where M is the mass of atom ^{87}Rb. $a_0 = 110a_{\mathrm{Bohr}}$ is s-wave scattering length, where a_{Bohr} is Bohr radius. The dimensionless gravity $G = (Mg/\hbar\omega_{1y})(\hbar/M\omega_{1y})^{1/2}$, where g is the gravitational acceleration. Δ is the detuning of the RF field from the resonant transition frequency at the center of the trap, and Ω is the Rabi frequency. The units of time, spatial coordinates, interaction strengths, and the wavefunctions are $1/\omega_{1y}$, $(\hbar/M\omega_{1y})^{1/2}$, $(\hbar\omega_{1y})^{-1}(\hbar/M\omega_{1y})^{-1/2}$, and $(\hbar/M\omega_{1y})^{-1/4}$, respectively.

For simulations in microgravity, G is zero. We use Gross–Pitaevskii Equation Laboratory (GPELab)[31] for our calculation with the Strang Alternate Direction Implicit-Time Splitting pseudo-Spectral (ADI-TSSP) scheme for dynamic evolution and spatial discretization/pseudo-spectral scheme (BESP) for ground state searching.

3. Results

Our simulation parameters are the same as those in Ref. [14]. The frequency of the trapped state $|F = 2, m_F = 2\rangle$ is $\omega_{\parallel} = 2\pi \times 225$ Hz and $\omega_{\perp} = 2\pi \times 20$ Hz. The offset magnetic field $V_{\mathrm{off}} = 1.5$ Gs (1 Gs = 10^{-4} T). Totally 5×10^4 atoms are in $|F = 2, m_F = 2\rangle$ at the beginning. The RF pulse duration is 24 μs.

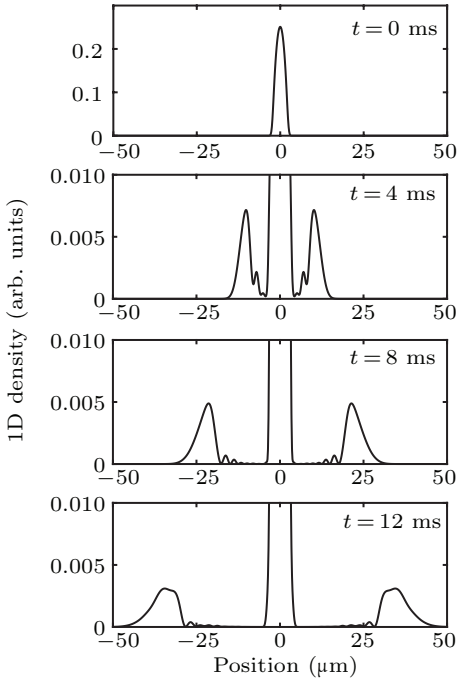


Fig. 1. The out-coupling process of pulsed atom laser in microgravity. Coupling strengths $\Omega = 1.5 \times 10^4$ Hz. The densities of $m_F = 1$, $m_F = 2$, and $m_F = 0$ states are shown. From top to bottom are density profiles at 0 ms, 4 ms, 8 ms, 12 ms respectively. The density profile in the center is the sum of density of $m_F = 1$, $m_F = 2$ states. The two symmetrical pulses are the output of atom lasers in $m_F = 0$ state.

In Fig. 1 we plot the density profiles before the 24-μs RF pulse, and after the RF pulse at moments 4 ms, 8 ms, 12 ms.

With $g = 0$, the gravitation sag is zero, thus the condensate's center is the magnetic trap center. Magnetically trapped states are oscillating around the equilibrium point after the RF pulse. The center peak in Fig. 1 is the sum of density of trapped states $|F = 2, m_F = 2\rangle$ and $|F = 2, m_F = 1\rangle$. The two symmetrical peaks are the atom laser output of untrapped state $|F = 2, m_F = 0\rangle$. The output atoms move in opposite directions due to the isotropic mean field repulsive interaction.[7] Without gravity, we can still see the cloud moving out due to the repelling force of the mean field interaction at the beginning. In contrast to the situation under gravity, where the gravity is asymmetric, the output atoms only move along the gravity. We can see interference pattern[18,19] in Fig. 1. Since the size of the pattern is several micrometers, these patterns are possible to be observed in experiments. From Fig. 1 we can get the velocity of atomic diffusion and the velocity of cloud center are about 5×10^{-4} m/s and 3×10^{-3} m/s, respectively.

In Fig. 2(a), the figures are density distribution profiles in microgravity at 0 ms, 2.5 ms, and 5 ms. In Fig. 2(b), the figures are density distribution profiles under gravity at 0 ms, 2.5 ms, and 5 ms respectively. Under gravity, the gravitation sag of trapped states is $Z = g/(|m|\omega_{1y}^2)$ while in microgravity there is no such sag. Here we shift the center of atom cloud to the same position in plots for comparison purpose. The untrapped state moves slowly in microgravity solely due to the repulsive interaction. The output laser pulse moves with a constant velocity after leaving the initial cloud. In contrast, output atoms move faster and faster in gravity due to gravity acceleration in Fig. 2(b). Note that all figures have the same scale in horizontal axis in Fig. 2. Slow output velocity means long interference time which is critical for precision measurements.

In Fig. 3, the evolution of trapped and untrapped states of atom laser after RF pulse at 0 ms, 3 ms, 6 ms, 9 ms, 12 ms are shown. The first row, second row, and third row are the density distribution of $|F = 2, m_F = 2\rangle$, $|F = 2, m_F = 1\rangle$, and $|F = 2, m_F = 0\rangle$ respectively. The width of output beam is increasing with time due to the mean field interaction effect. Besides, the state $|F = 2, m_F = 1\rangle$ has the same equilibrium position with the state $|F = 2, m_F = 2\rangle$. We can see the trapped states are oscillating around the center of the trap. The $|F = 2, m_F = 1\rangle$ state has larger oscillation amplitude due to smaller trapping frequency compared with state $|F = 2, m_F = 2\rangle$. Most atoms are still in $|F = 2, m_F = 2\rangle$ state in our simulations. The profile of atoms in $|F = 2, m_F = 2\rangle$ does not change dramatically because the interaction strength from other states is small. For atoms in $|F = 2, m_F = 1\rangle$ state, they always feel a strong interaction from $|F = 2, m_F = 2\rangle$ state in the central region. Although there are complicated dynamics for trapped atoms, $|F = 2, m_F = 0\rangle$ atoms just freely expand after they leave the central region.

Output flux can be adjusted by varying the coupling strengths. Too strong coupling strengths would shut down atom laser[32–34] due to the existence of the stationary bound mode. For weak coupling, the output flux increases as coupling strengths increases.[35,36] As can be seen in Fig. 4, the coupling strengths are 2×10^3 Hz, 7×10^3 Hz, 9×10^3 Hz, 1.5×10^4 Hz from top to bottom. The peak density of untrapped state increases drastically as the coupling strengths increases. For relatively weak coupling strengths the distribution profiles are almost the same. The slight difference at different coupling strengths is due to the different interaction strengths which is a function of atom numbers. The stronger coupling strength makes the atom number in trapped states smaller, which makes the repulsive potential smaller. This is the reason why the output pulse goes a shorter distance for stronger coupling. In stronger coupling case, the atom laser pulse is broader due to larger repulsive interaction of itself.

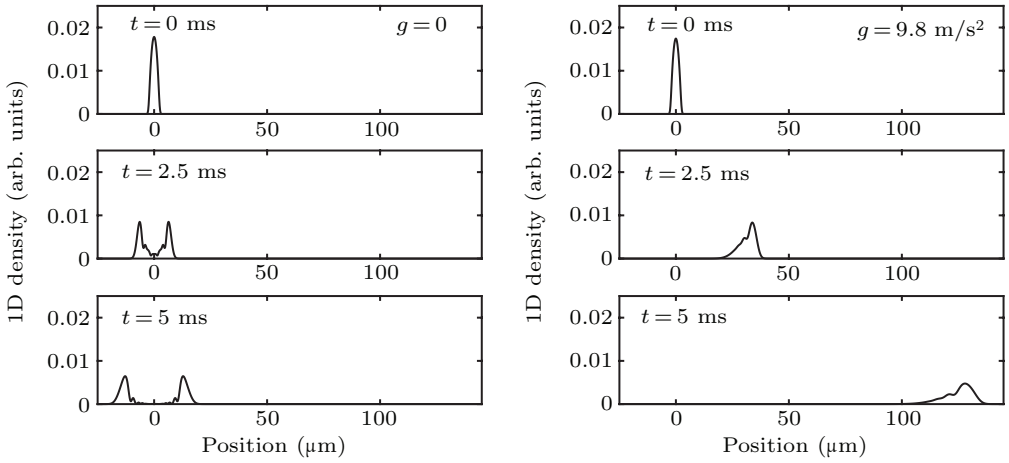


Fig. 2. The comparison of atom laser outputs between in microgravity and in gravity, $\Omega = 1.5 \times 10^4$ Hz. (a) The out-coupling process in microgravity when $g = 0$. From top to bottom the density profiles are at 0 ms, 2.5 ms, and 5 ms respectively. (b) The out-coupling process under gravity when $g = 9.8$ m/s^2. The density profiles are at the same moments as in panel (a). Note that all figures have the same scale in horizontal axis.

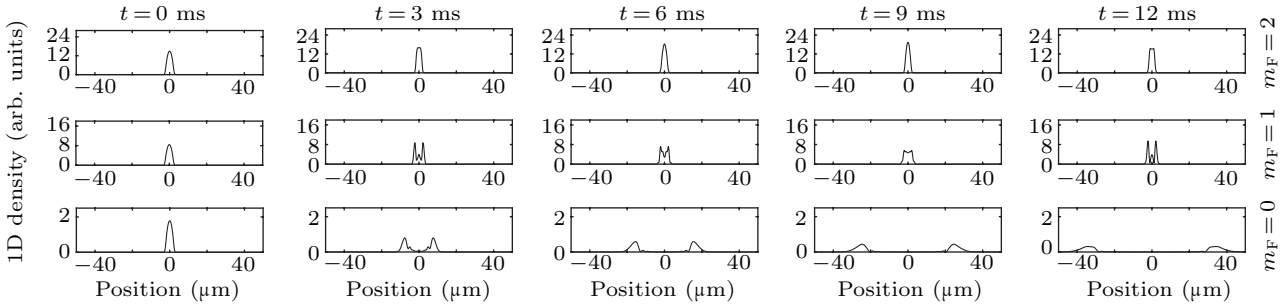


Fig. 3. Out-coupling process of pulse atom laser in microgravity, $\Omega = 1.5 \times 10^4$ Hz. From left to right the density profiles at 0 ms, 3 ms, 6 ms, 9 ms, and 12 ms are shown. The rows from top to bottom represent $m_F = 2$, $m_F = 1$, and $m_F = 0$ components. Other parameters are the same as those in Fig. 1.

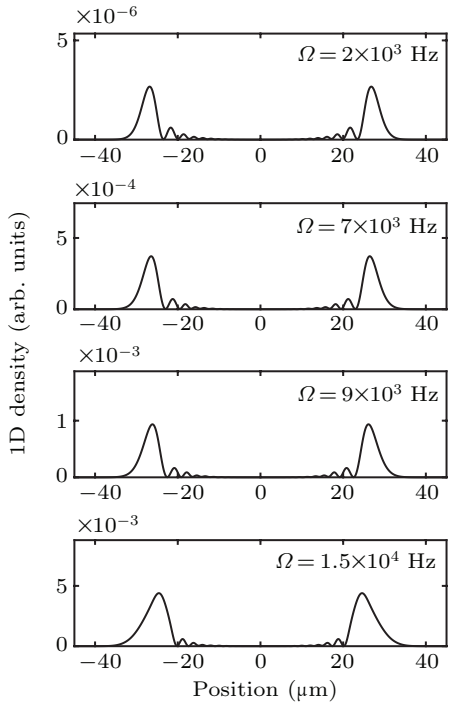


Fig. 4. The out-coupling with different coupling strengths. The density distribution of $m_F = 0$ state at 9 ms are shown with different coupling strengths. From top to bottom the coupling strengths Ω are 2×10^3 Hz, 7×10^3 Hz, 9×10^3 Hz, and 1.5×10^4 Hz respectively. Other parameters are the same as those in Fig. 1.

The atom number and trapping frequency of the simulations in this work are close to the experimental parameters in the space lab.[1] Totally 1.3×10^5 atoms including thermal clouds can be created at the final cooling stage in Ref. [1]. We use 5×10^4 atoms in the simulations. The typical trapping frequencies are $2\pi \times (310, 1450, 1570)$ Hz in Ref. [1], and the frequencies can be adjusted in large range.[1] We use $2\pi \times 225$ Hz along the 1D direction. Our experience is that the simulations will not change qualitatively within a large range of parameters.

4. Conclusion and perspectives

In conclusion, we have simulated the dynamics of the pulsed atom laser of the $F = 2$ manifold both in microgravity and under gravity in one dimension. One distinct property of 1D atom laser in microgravity is double pulses output in opposite directions after a single RF pulse coupling. The other property is the slow moving velocity of atom laser. The slow moving velocity leads to long interference time which is important for precision measurements. The output flux changes drastically as the coupling strength changes, with which one can manipulate atom laser population in microgravity.

References

[1] Aveline D C, Williams J and Elliott E 2020 *Nature* **582** 193
[2] Liu L, Lü D S, Chen W B, Li T, Qu Q Z, Wang B, Li L, Ren W, Dong Z R, Zhao J B, Xia W B, Zhao X, Ji J W, Ye M F, Sun Y G, Yao Y Y, Song D, Liang Z G, Hu S J, Yu D H, Hou X, Shi W, Zang H G, Xiang J F, Peng X K and Wang Y Z 2018 *Nat. Commun.* **9** 2760
[3] Müntinga H, Ahlers H, Krutzik M, Wenzlawski A, Arnold S, Becker D, Bongs K, Dittus H, Duncker H, Gaaloul N, Gherasim C, Giese E, Grzeschik C, Hänsch T W, Hellmig O, Herr W, Herrmann S, Kajari E, Kleinert S, Lämmerzahl C, Lewoczko-Adamczyk W, Malcolm J, Meyer N, Nolte R, Peters A, Popp A, Reichel J, Roura A, Rudolph J, Schiemangk M, Schneider M, Seidel S T, Sengstock K, Tamma V, Valenzuela T, Vogel A, Walser R, Wendrich T, Windpassinger P, Zeller W, Zoest T V, Ertmer W, Schleich W P and Rasel E M 2013 *Phys. Rev. Lett.* **110** 093602
[4] Becker D, Lachmann M D, Windpassinger P and Rasel E M 2018 *Nature* **562** 391
[5] Li C, Zhou T, Zhai Y, Xiang J, Luan T, Huang Q, Xiong W and Chen X Z 2017 *Rev. Sci. Instrum.* **88** 053104
[6] Luan T, Li Y, Zhang X and Chen X Z 2018 *Rev. Sci. Instrum.* **89** 123110
[7] Matthias M, Albert R, Rasel E M and Schleich W P 2019 *New J. Phys* **21** 013039
[8] Tononi A, Cinti F and Salasnich L 2020 *Phys. Rev. Lett.* **125** 010402
[9] Tononi A and Salasnich L 2019 *Phys. Rev. Lett.* **123** 160403
[10] Lundblad N, Carollo R A, Lannert C, Gold M J, Jiang X, Paseltiner D, Sergay N and Aveline C 2019 *npj Microgravity* **5** 30
[11] Padavić K, Sun K, Lannert C and Vishveshwara S 2020 *Phys. Rev. A* **102** 043305
[12] Mewes M O, Andrews M R, Kurn D M, Durfee D S, Townsend C G and Ketterle W 1997 *Phys. Rev. Lett.* **78** 582
[13] Robins N P, Savage C M, Hope J J, Lye J E, Fletcher C S, Haine S A and Close J D 2004 *Phys. Rev. A* **69** 051602
[14] Xia L, Yang F, Zhou X and Chen X Z 2009 *Phys. Lett. A* **373** 1429
[15] DugúeJ, Robins N P, Figl C, Jeppesen M, Summers P, Johnsson M T, Hope J J and Close J D 2007 *Phys. Rev. A* **75** 053602
[16] Coq Y L, Thywissen J F, Rangwala S A, Gerbier F, Richard S, Delannoy G, Bouyer P and Aspect A 2001 *Phys. Rev. Lett.* **87** 170403
[17] Öttl A, Ritter S, Köhl M and Esslinger T 2005 *Phys. Rev. Lett.* **95** 090404
[18] Köhl M, Hänsch T W and Esslinger T 2001 *Phys. Rev. Lett.* **87** 160404
[19] Bloch I, Hansch T W and Esslinger T 2000 *Nature* **403** 166
[20] Xia L, Xiong W, Wang F, Yi L, Zhou X J and Chen X Z 2008 *Chin. Phys. Lett.* **25** 2374
[21] Liu X J, Jing H and Ge M L 2006 *Chin. Phys. Lett.* **23** 1184
[22] Qin J L 2019 *Chin. Phys. B* **28** 126701
[23] Rolston S and Phillips W N 2002 *Nature* **416** 219

[24] Büning G K, Will J, Ertmer W, Klempt C and Arlt J 2010 *Appl. Phys. B* **100** 117
[25] Zoest T V, Gaaloul N, Singh T, Ahlers H, Herr W, Seidel S T, Ertmer W, Rasel E, Eckart M, Kajari E, Arnold S, Nandi G, Schleich W P, Walser R, Vogel A, Sengstock K, Bongs K, Lewoczko-Adamczyk W, Schiemangk M, Schuldt T, Peters A, Könemann T, Müntinga H, Lämmerzahl C, Dittus H, Steinmetz T, Hänsch T W and Reiche 2010 *Science* **328** 1540
[26] Kinoshita T, Wenger T R and Weiss D S 2004 *Science* **305** 1125
[27] Paredes B, Widera A and Murg V 2004 *Nature* **429** 277
[28] Wilson J M, Malvania N, Le Y, Zhang Y, Rigol M and Wesis D S 2020 *Science* **367** 1461
[29] Kinoshita T, Wenger T and Weiss D S 2006 *Nature* **440** 900
[30] Schneider J and Schenzle A 1999 *Appl. Phys. B* **69** 353
[31] Antoine X and Duboscq R 2014 *Comput. Phys. Commun.* **185** 2969
[32] Robins N, Altin P, Debs J and Close J 2013 *Phys. Rep.* **529** 265
[33] Jeffers J, Horak P, Barnett S M and Radmore P M 2000 *Phys. Rev. A* **62** 043602
[34] Hope J J, Moy G M, Collett M J and Savage C M 2000 *Phys. Rev. A* **61** 023603
[35] Robins N P, Morrison A K, Hope J J and Close J D 2005 *Phys. Rev. A* **72** 031606(R)
[36] Steck H, Naraschewski M and Wallis H 1998 *Phys. Rev. Lett.* **80** 1